Characterization of rainfall distribution and flooding associated with U.S. landfalling tropical cyclones: Analyses of Hurricanes Frances, Ivan, and Jeanne (2004)

Gabriele Villarini,[1,2] James A. Smith,[1] Mary Lynn Baeck,[1] Timothy Marchok,[3] and Gabriel A. Vecchi[3]

Received 28 April 2011; revised 27 September 2011; accepted 28 September 2011; published 14 December 2011.

[1] Rainfall and flooding associated with landfalling tropical cyclones are examined through empirical analyses of three hurricanes (Frances, Ivan, and Jeanne) that affected large portions of the eastern U.S. during September 2004. Three rainfall products are considered for the analyses: NLDAS, Stage IV, and TMPA. Each of these products has strengths and weaknesses related to their spatio-temporal resolution and accuracy in estimating rainfall. Based on our analyses, we recommend using the Stage IV product when studying rainfall distribution in landfalling tropical cyclones due to its fine spatial and temporal resolutions (about 4-km and hourly) and accuracy, and the capability of estimating rainfall up to 150 km from the coast. Lagrangian analyses of rainfall distribution relative to the track of the storm are developed to represent evolution of the temporal and spatial structure of rainfall. Analyses highlight the profound changes in rainfall distribution near landfall, the changing contributions to the rainfall field from eyewall convection, inner rain bands and outer rain bands, and the key role of orographic amplification of rainfall. We also present new methods for examining spatial extreme of flooding from tropical cyclones and illustrate the links between evolving rainfall structure and spatial extent of flooding.

Citation: Villarini, G., J. A. Smith, M. L. Baeck, T. Marchok, and G. A. Vecchi (2011), Characterization of rainfall distribution and flooding associated with U.S. landfalling tropical cyclones: Analyses of Hurricanes Frances, Ivan, and Jeanne (2004), *J. Geophys. Res.*, *116*, D23116, doi:10.1029/2011JD016175.

1. Introduction

[2] Landfalling tropical cyclones dominate the upper tail of flood peak distribution in large areas of the eastern U.S. [*Villarini and Smith*, 2010], with flood peak properties that are closely linked to the spatial and temporal distribution of rainfall [*Smith et al.*, 2011; *Villarini and Smith*, 2010]. Previous studies have examined rainfall distribution from landfalling tropical cyclones in the U.S. *Atallah et al.* [2007] present a "general paradigm for understanding the dynamics responsible for modulating the distribution, spatial extent, location, and intensity of precipitation associated with tropical cyclones subsequent to landfall."

[3] Prediction of precipitation and flooding associated with landfalling tropical cyclones is of paramount importance from a societal and economic point of view [e.g., *Rappaport*, 2000; *Pielke et al.*, 2008; *Changnon*, 2009] and represents a major challenge [*Elsberry*, 2002]. The AMS policy statement on hurricane research and forecast note that "skillful prediction of rainfall from landfalling tropical cyclones remains elusive" and "rainfall prediction remains highly subjective" [*American Meteorological Society* (*AMS*), 2000].

[4] While the vast majority of the studies focus on analyses and modeling of rainfall associated with landfalling tropical cyclones [e.g., *Rao and MacArthur*, 1994; *Cerveny and Newman*, 2000; *Ferraro et al.*, 2005; *Kidder et al.*, 2005; *Tuleya et al.*, 2007; *Lonfat et al.*, 2007; *Atallah et al.*, 2007; *Jiang et al.*, 2008b; *Ebert et al.*, 2011], the examination of flooding from these storms from a regional perspective has received very little attention [*Sturdevant-Rees et al.*, 2001; *Smith et al.*, 2011], despite the large impacts that freshwater floods from tropical cyclones have [*Rappaport*, 2000]. In general, we would expect heavy rainfall to be a key ingredient for flooding. This is not, however, a sufficient or necessary condition as the flood extent and magnitude depend also on land use/land cover properties and soil saturation [e.g., *Hellin et al.*, 1999; *Sturdevant-Rees et al.*, 2001]. In this paper, we develop techniques for representing the spatial and temporal evolution of rainfall relative to the center of circulation of the storm, and the regional extent of flooding associated with landfalling tropical cyclones.

[5] A realistic characterization of heavy rainfall and flooding from landfalling tropical cyclones should account not

[1]Department of Civil and Environmental Engineering, Princeton University, Princeton, New Jersey, USA.
[2]Willis Research Network, London, UK.
[3]Geophysical Fluid Dynamics Laboratory, National Oceanic and Atmospheric Administration, Princeton, New Jersey, USA.

0148-0227/11/2011JD016175

only for the large scale environmental conditions but also for local factors (e.g., pervious versus impervious areas, significant orography). We need, therefore, to move away from at-site or point representation of these processes and into the realm of "spatial extremes" [see *Smith et al.*, 2011]. The term "spatial extremes" underlies both the extreme nature of these events as well their intrinsic spatially coherent nature.

[6] From a modeling standpoint, it is much easier to deal with univariate at-site description of rainfall and flooding. Including the intrinsic spatial correlation and the local drivers of heavy rainfall and flooding, and accounting for the anthropogenic changes (e.g., construction of dams) that these catchments have undergone during the twentieth century [e.g., *Villarini and Smith*, 2010] would result in adopting a framework that is currently at the forefront of the statistical literature [e.g., *Padoan et al.*, 2010] and needs to develop further before we will be able to apply it in this very complex context. While these data could represent a valuable test bed for these statistical models, a data-driven approach could, on the other hand, represent a viable alternative to models based on inference of spatial extremes. This methodology would build on the wealth of discharge and rainfall data available in the U.S. Discharge data have been collected, archived and published by the US Geological Survey (USGS) starting from the nineteenth century. Rainfall data are available for a comparable period of time. Rain gage measurements are archived by the National Climatic Data Center (NCDC) and new reanalysis data sets are available for the 20th century [*Compo et al.*, 2006, 2011]. For more recent periods, gridded rainfall fields are derived from rain gages, ground-based weather radars, and satellite sensors.

[7] In this study we perform analyses concerning the feasibility of a data-driven rainfall model for U.S. landfalling tropical cyclones. The main goals of this paper are (1) analysis of spatial extremes of rainfall and flooding for a sequence of hurricanes in 2004 (Frances, Ivan, and Jeanne); (2) development and demonstration of data analysis procedures for characterization of rainfall distribution as a function of distance from the center of circulation; and (3) comparison of three rainfall products (North American Land Data Assimilation System (NLDAS), Stage IV, and Tropical Rainfall Measuring Mission (TRMM) Multiple Satellite Precipitation Analysis (TMPA)) for three hurricanes making landfall along the coast of the U.S. in 2004 (Frances, Ivan, and Jeanne).

[8] Numerous studies have examined the distribution of rainfall associated with over-land and over-ocean tropical cyclones using different precipitation data sets (see *Kimball* [2008] for results from an idealized landfalling hurricane model). In general, over-the-ocean the radial distribution of azimuthally averaged rainfall tends to increase up to 50–100 km from the center of circulation and then to decrease for increasing radial distance [e.g., *Rodgers and Adler*, 1981; *Rodgers et al.*, 1994; *Rodgers and Pierce*, 1995; *Jiang et al.*, 2008b; *Yokoyama and Takayabu*, 2008]. The rainfall distribution changes over land with the maximum rainfall that tends to be at the center of circulation and then decreases for increasing distance [e.g., *Marchok et al.*, 2007; *Kimball*, 2008; *Jiang et al.*, 2008b; *Tuleya et al.*, 2007; *Yokoyama and Takayabu*, 2008]. *Jiang et al.* [2008b] analyzed a total of 37 tropical cyclones using rainfall estimates obtained from the TMPA product. They stratified the data according to different tropical cyclone intensities and whether the storms were over oceans, over land, or mixed. *Langousis and Veneziano* [2009a, 2009b] proposed a physical-statistical model of tropical cyclone rainfall for open water sites but not accounting for landfall effects. *Lonfat et al.* [2004] analyzed instantaneous precipitation observations from the TRMM Microwave Imager (TMI) over six ocean basins for the period 1998–2000. Other studies [e.g., *Colle*, 2003; *Atallah and Bosart*, 2003] examined heavy rainfall distribution in tropical cyclones after they underwent extra-tropical transition using both observations and numerical models.

[9] Satellite-based rainfall estimates represent a valuable source of information in areas of the globe where no information from ground-based stations is available, in particular over oceans. However, their spatial and temporal resolutions (on the order of three hours and 0.25-degree) or infrequent sampling (once or twice a day), together with the uncertainties associated with these rainfall estimates, represent a significant drawback in studies examining the spatial and temporal evolution of tropical cyclones at landfall.

[10] Ground-based weather radar data represent a viable alternative to satellite-based rainfall estimates. They are characterized by higher spatial and temporal resolutions (5 minutes and about 1-km horizontal resolution) and have already been used to study rainfall and flooding in landfalling tropical cyclones [e.g., *Glitto and Choy*, 1997; *Blackwell*, 2000; *Sturdevant-Rees et al.*, 2001; *Medlin et al.*, 2007; *Curtis et al.*, 2007; *Matyas*, 2009; *Javier et al.*, 2010; *Villarini et al.*, 2010]. Radar data, however, are affected by several sources of uncertainties (consult *Villarini and Krajewski* [2010] for a recent review) and a radar can cover only a limited region (on the order of 150 km) in open water before the storm makes landfall.

[11] Rain gages represent the most direct and accurate way of measuring rainfall. Their main drawback is that their measurements represent only a limited area around the instrument and there are very few specialized networks dense enough to capture the rainfall spatial variability. Moreover, there is no information available prior to landfall [e.g., *Matyas and Cartaya*, 2009].

[12] This paper is organized as follows. The three rainfall products (NLDAS, TMPA, and Stage IV) are described in Section 2, together with a summary of the characteristics of three hurricanes (Frances, Ivan and Jeanne). Section 3 describes the results of our analyses. A summary and conclusions are presented in Section 4.

2. Rainfall Data and Storm Summary

[13] The Stage IV multisensor rainfall product is generated by National Oceanic and Atmospheric Administration (NOAA) National Centers for Environmental Prediction (NCEP) [*Baldwin and Mitchell*, 1998; *Lin and Mitchell*, 2005]. At its finest scale, it represents hourly accumulations over the Hydrologic Rainfall Analysis Project (HRAP) grid (about 4-km pixels [e.g., *Reed and Maidment*, 1999]). It is mosaicked over the continental U.S. and a few thousand rain gages are used to bias correct this product [*Lin and Mitchell*, 2005]. This product has been used as a reference

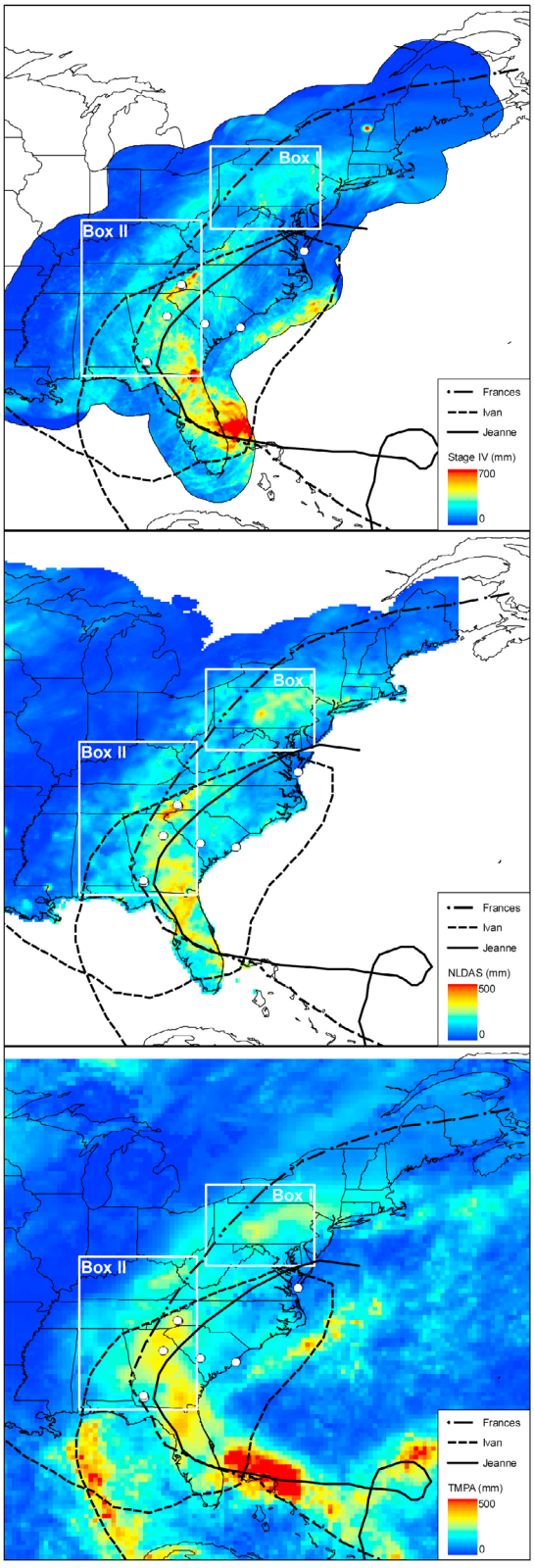

Figure 1. Storm total accumulation for the month of September 2004 based on (top) Stage IV, (middle) NLDAS, and (bottom) TMPA. Note that the range of values for the Stage IV storm total is different from those for the other two rainfall products. The white circles indicate the location of the USCRN rain gages used to evaluate the Stage IV data.

in studies examining storm total rainfall for landfalling tropical cyclones [e.g., *Ferraro et al.*, 2005; *Lonfat et al.*, 2007; *Marchok et al.*, 2007; *Jiang et al.*, 2008a].

[14] The NLDAS rainfall product [*Mitchell et al.*, 2004] is based principally on rain gage observations. The daily measurements from rain gages are disaggregated to the hourly scale using the information provided by the Stage IV rainfall data about the temporal evolution of the precipitation systems. It is a gridded product available at the hourly scale and with a spatial resolution of 1/8 degree lat/lon (approximately 12.5-km pixels) over the continental U.S.

[15] The TMPA product is generated by merging both infrared and passive microwave satellite observations [*Huffman et al.*, 2007]. In its research version, the TMPA monthly accumulations are scaled to match the monthly rain gage observations. This product is available at the three-hourly scale averaged over a 1/4 degree lat/lon pixel (about 25-km pixels). The data cover a tropical and midlatitude belt between 50° north and 50° south.

[16] The North Atlantic hurricane season of 2004 was one of most active in the record. There were fifteen named storms, nine hurricanes, six of which became major hurricanes, with an overall activity above average. These storms resulted in 3100 fatalities, 60 of which were in the U.S. The property damages in the U.S. was about $45 billion, with Ivan, Frances, and Jeanne ranking in the top ten highest hurricane losses during the period 1949–2006 [*Changnon*, 2009]. For the first time in the US hurricane record, four hurricanes made landfall in Florida. For a detailed description of the 2004 hurricane season, consult *Franklin et al.* [2006].

[17] In this study we focus on three of these hurricanes: Frances, Ivan, and Jeanne, all making landfall in the U.S. during September 2004. Frances, a hurricane of the Cape Verde-type, developed on August 21st off the African Coast. At its peak, it reached Cat 4 intensity (maximum sustained wind speed exceeding 58 m s^{-1}) and made landfall in Florida as a Cat 2 (maximum sustained wind speed exceeding 43 m s^{-1}) hurricane (see Figure 1 for the best track). The lowest pressure and maximum sustained wind recorded by a land station was 948.1 mb and approximately 45 m s^{-1}. Eight fatalities were directly associated with Frances. Of these fatalities, seven were in the U.S. (five in Florida, and one each in Georgia and Ohio), related to wind (three), storm surge (one) freshwater floods (one), tornado (one) and lightning (one). The total U.S. economic damage was approximately $9 billion, while the insured damage was approximately $4.4 billion, most of which in Florida.

[18] Like Frances, Ivan was a Cape Verde-type hurricane and developed on August 31st off the coast of Africa. It reached Cat 5 (maximum sustained wind speed exceeding 69 m s^{-1}) intensity three times, making landfall as a Cat 3 (maximum sustained wind speed exceeding 50 m s^{-1}; see Figure 1 for the best track). The lowest pressure was 910 mb and the maximum sustained wind was estimated to be approximately 75 m s^{-1}. The number of fatalities directly caused by Ivan was 92, of which 25 were in the U.S. The U.S. state with the largest toll was Florida with 14, followed by North Carolina with eight, Georgia with two and Mississippi with one. Of the 25 U.S. fatalities, seven were caused by tornadoes, five by storm surge, four by freshwater floods, four by mud slides, three by wind, and

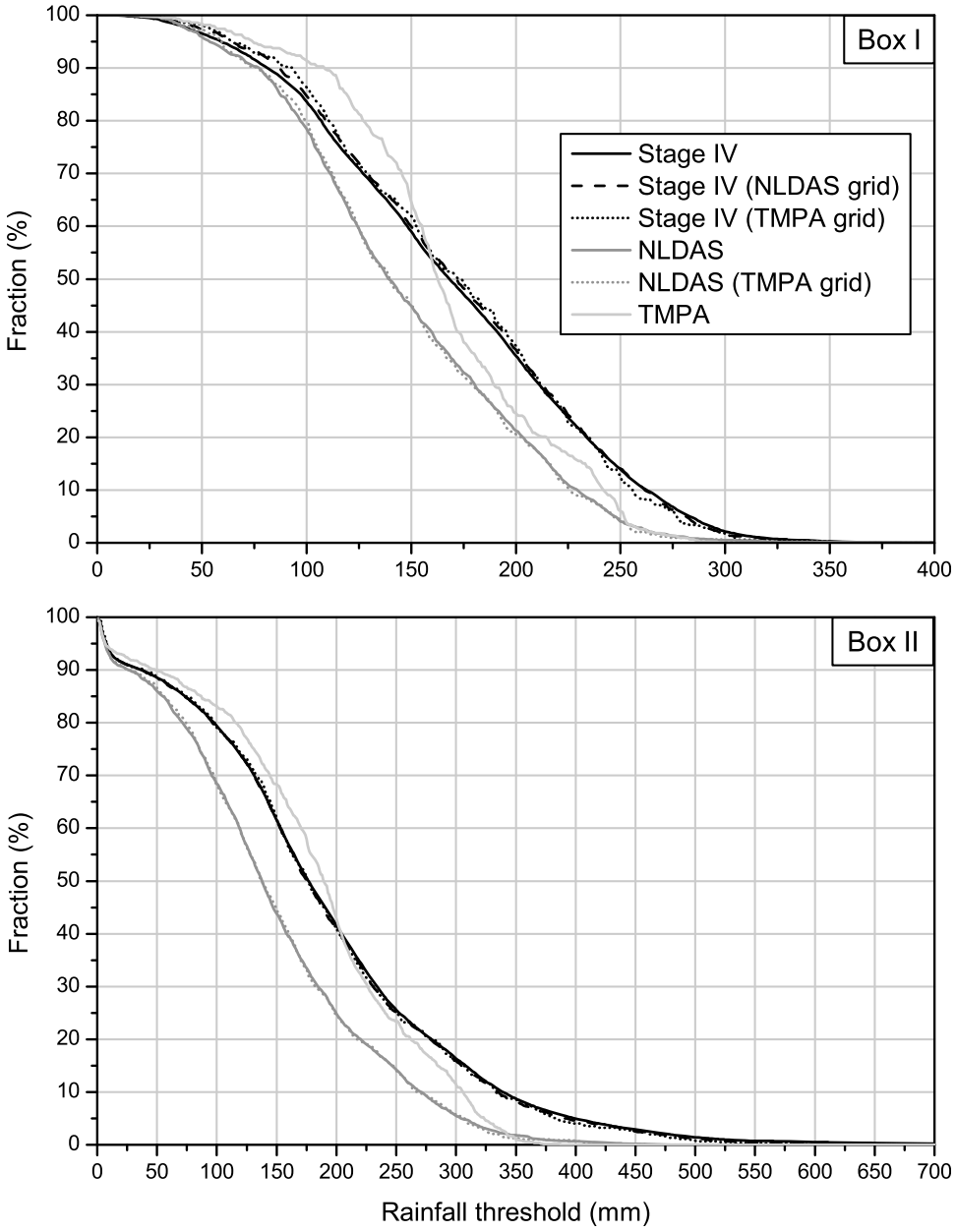

Figure 2. Percentage of pixels exceeding a certain rainfall threshold for (top) Box I and (bottom) Box II. The location of Boxes I and II is shown in Figure 1.

two by surf. Ivan was responsible for over $14 billion in economic damage in the U.S., with over $7 billion in insured losses.

[19] Jeanne originated as a tropical wave, moving from Africa on September 7th. It reached Cat 3 intensity at its peak, which is also the category at which it made landfall in Florida (see Figure 1 for the best track). The lowest pressure is estimated to have been 950 mb, with an estimated maximum sustained wind of 54 m s^{-1}. Over 3000 fatalities were reported in Haiti, most of which caused by mud slides. In the U.S., six fatalities were a direct consequence of Jeanne, three of which were in Florida, and one in Puerto Rico, Virginia, and South Carolina. The estimated total economic damage for the U.S. was $6.9 billion, with estimated insurance properties losses of $3.5 billion.

3. Results

3.1. Intercomparison of Rainfall Products

[20] To highlight some of the strengths and weaknesses of these products, we can refer to Figure 1, where we show the rainfall accumulation for the month of September 2004 for the three different rainfall products (Stage IV: top panel; NLDAS: middle panel; bottom panel: TMPA). The largest accumulation values occur along the Florida peninsula and along the Appalachian Mountains, in particular in North

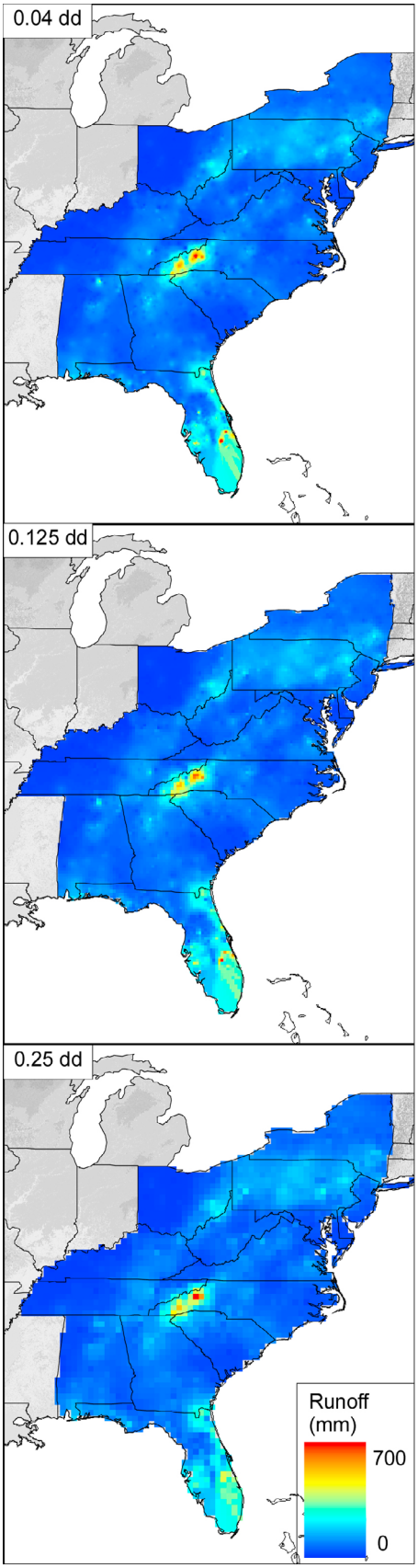

Carolina. We have large rainfall accumulations out to the Atlantic Ocean, in particular on the eastern side of Florida and the coast of the Carolinas. When using rainfall estimates obtained from the NLDAS and TMPA, the areas with the largest accumulations tend to be similar across these different products. The rainfall values tend to be smaller for coarser resolution products and we also lose some of the spatial details available at finer scales. The Stage IV product has the highest spatial resolution (approximately 4-km pixels), which provides capability to resolve spatial features of rainfall in greater detail. Going from Stage IV to NLDAS to TMPA, the largest rainfall accumulations are found in the Florida peninsula and the southern part of the Appalachian Mountains. The rainfall maximum in the Appalachian Mountains (North Carolina), however, is increasingly smoothed going from a product with a 4-km pixel to one with a 25-km pixel. These results highlight the importance of a high spatial resolution to capture the spatial variability of rainfall associated with a landfalling tropical cyclone [see, e.g., *Lin et al.*, 2010]. Moreover, the differences in rainfall estimates across the various products are not limited to the different spatial resolutions, but also to the different data on which they are based (weather radar, rain gage, satellite), as well as to the different methodologies used to merge the rainfall data.

[21] To investigate whether the different accumulation values could be due to the different spatial resolutions, we focus on Box I and Box II in Figure 1 and compute the fraction of pixels above specified thresholds (Figure 2). We regridded the Stage IV data to a coarser resolution (0.125- and 0.25-degree) by averaging all the Stage IV pixels with centers falling within a given pixel of the coarser grid (for more sophisticated approaches, consult *Jones* [1999]). Based on these results, we infer that pixel size does not plays a large role in explaining the differences among these three products, but the regridding method used in this study could affect the very large rainfall values [e.g., *Jones*, 1999]. Comparing the results for the two boxes, we see a consistent picture. The Stage IV product has the largest fraction of pixels larger than 150 mm. Even after aggregating the results to the NLDAS and TMPA scales, the picture remains largely unchanged. Compared to the Stage IV, the TMPA data show a larger (smaller) fraction of pixels below (above) about 150 mm. On the other hand, NLDAS exhibits the lowest fraction of values independently of the rainfall threshold. This is also reflected in the average values within each box. The average rainfall for Box I based on Stage IV is 170.4 mm, on NLDAS is 147.5 mm, and on TMPA is 167.4 mm. For Box II, the average rainfall values are 190.2 mm (Stage IV), 146.5 mm (NLDAS), and 183.6 mm (TMPA).

[22] As a possible way to assess whether Stage IV is biased high or NLDAS biased low, we can use discharge data and consider the catchments as "glorified" rain gages. The runoff values provide a lower bound on rainfall. We used 2096 U.S. Geological Survey (USGS) stations and

Figure 3. Map of September 2004 runoff (mm) derived from 2096 USGS observations interpolated at three different aggregation scales: (top) 0.04 decimal degrees, (middle) 0.125 decimal degrees, and (bottom) 0.25 decimal degrees). Interpolation is performed using the inverse distance weighting method.

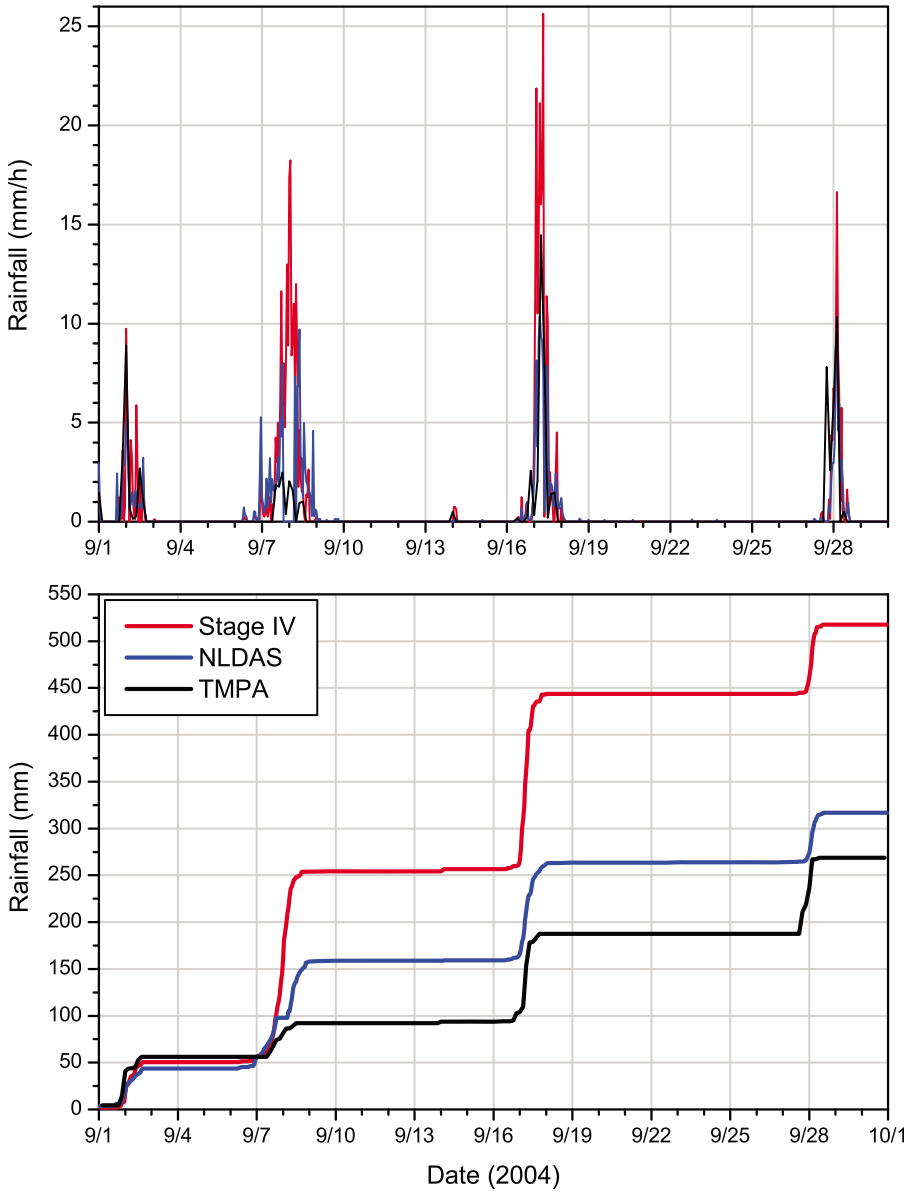

Figure 4. (top) Time series plot and (bottom) cumulative rainfall for a 0.25-degree pixel during September 2004 based on Stage IV, NLDAS, and TMPA.

transform the discharge time series for September 2004 from $m^3\ s^{-1}$ into runoff in mm by integrating discharge over time and normalizing by the drainage area (Figure 3). We have interpolated the runoff data at three spatial resolutions reflecting the resolution of the three rainfall products. Runoff is particularly large in western North Carolina, where we have values larger than 700 mm. This is also a region with large rainfall accumulations according to all the products (Figure 1). The rainfall accumulations for the NLDAS and TMPA are, however, smaller than the runoff values, while the Stage IV values are of comparable magnitude. These results provide additional evidence of the importance of spatial resolution in the Stage IV rainfall accumulations.

[23] To further examine the capability of these products to capture not only the spatial but also the temporal variability of rainfall from tropical cyclones, we focus on a 0.25-degree pixel in western North Carolina, the region with runoff values on the order of 500 mm (Figure 3). Figure 4 highlights similarities but also differences in the rainfall temporal variability among these products. They all clearly detect significant rainfall during the three hurricanes, and the timing of the peak rainfall matches well. Even the temporal distribution is well represented. There are, however, large discrepancies when it comes to rainfall magnitude. Stage IV has the largest rainfall values, followed by NLDAS. Overall, TMPA exhibits the smallest rainfall values. These differences become clearer when we examine the progressive accumulation for September 2004 (Figure 4, bottom). The rainfall accumulation for Frances is on the order of 200 mm for Stage IV, while it is much smaller for the other two products. This holds for Ivan as well. On the other hand, all the products have comparable rainfall accumulations for Jeanne. To

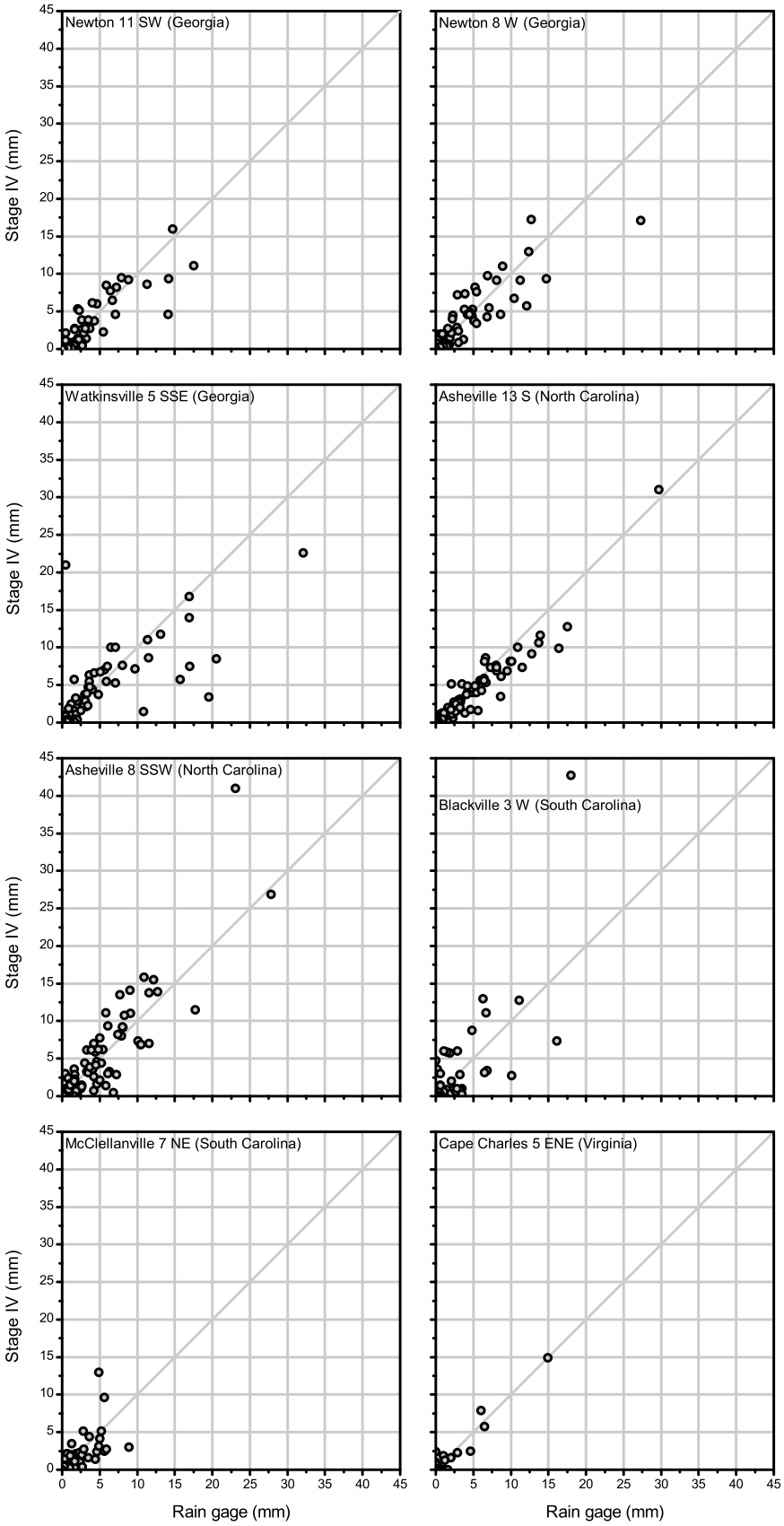

Figure 5. Scatterplots between rain gage and Stage IV rainfall at the hourly scale. The location of the rain gage stations is shown in Figure 1.

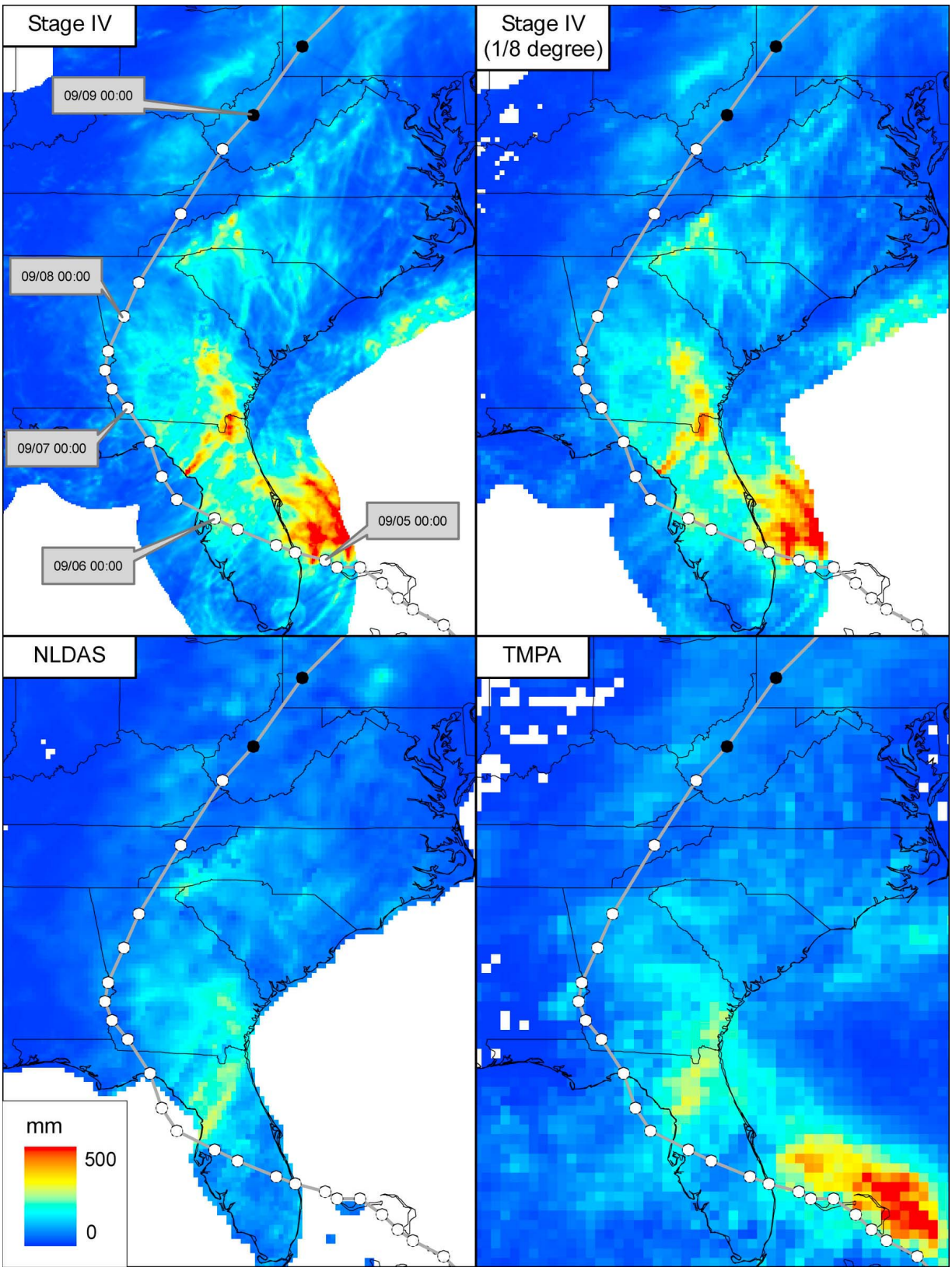

Figure 6. Rainfall accumulation for Hurricane Frances (over the period September 3–11 2004) based on (top left) Stage IV, (top right) Stage IV resampled to 1/8 degree-resolution, (bottom left) NLDAS, and (bottom right) TMPA. The dots represent the location of the center of circulation of the storm (the black dots indicate that the storm is extra-tropical).

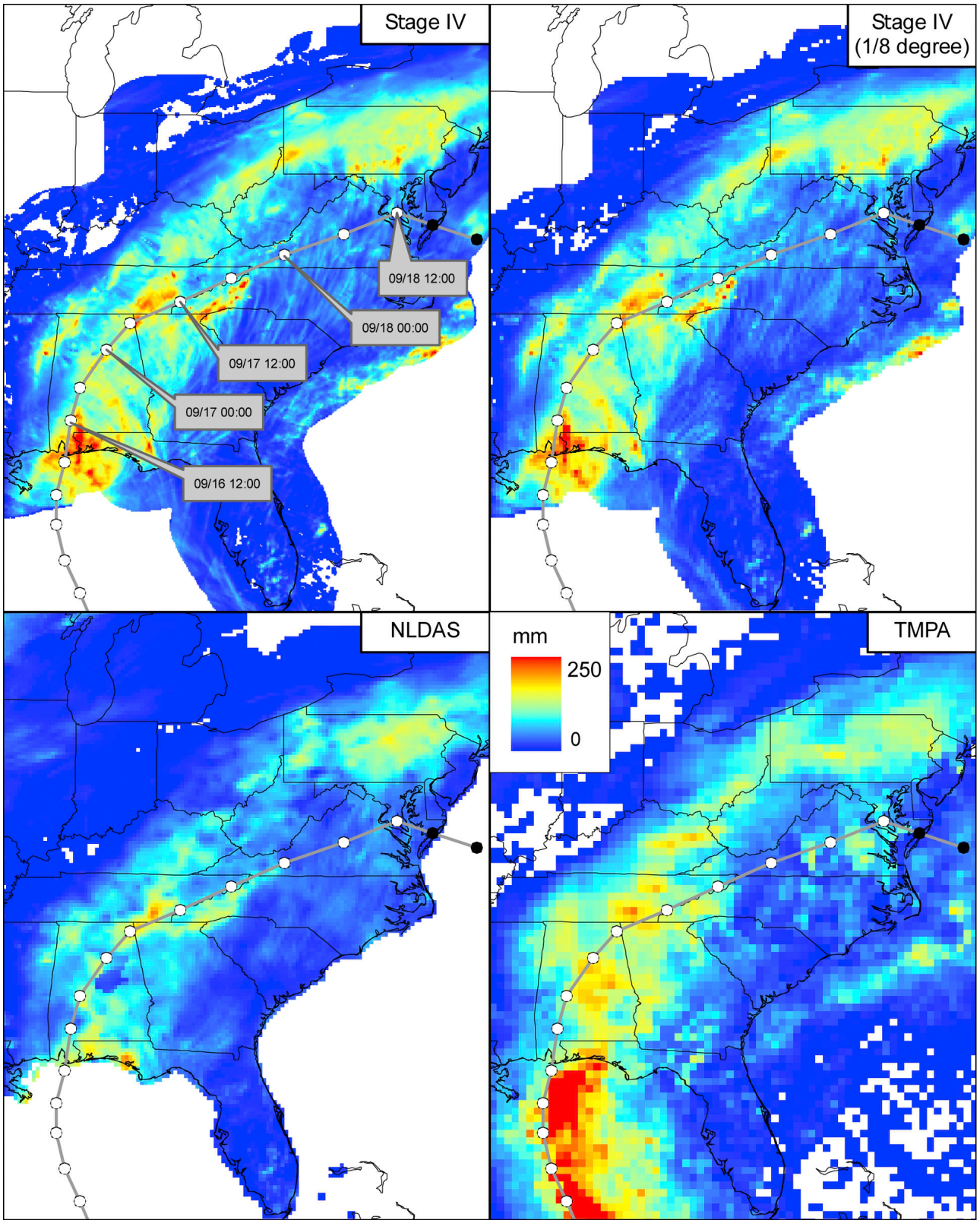

Figure 7. Rainfall accumulation for Hurricane Ivan (over the period September 13–18 2004) based on (top left) Stage IV, (top right) Stage IV resampled to 1/8 degree-resolution, (bottom left) NLDAS, and (bottom right) TMPA. The dots represent the location of the center of circulation of the storm (the black dots indicate that the storm is extra-tropical). The storm track is shown until September 19 at 0 UTC.

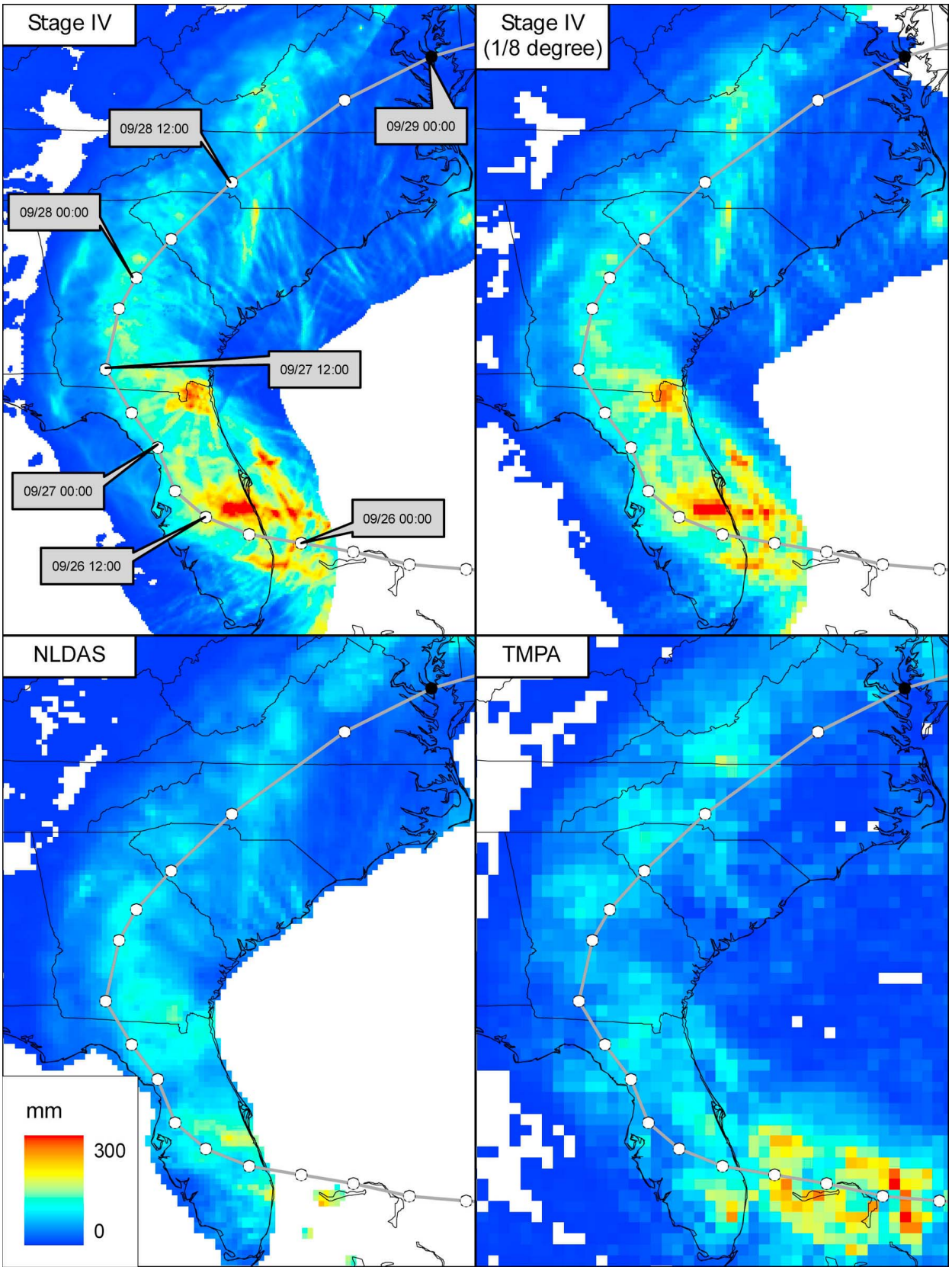

Figure 8. Rainfall accumulation for Hurricane Jeanne (over the period September 25–30 2004) based on (top left) Stage IV, (top right) Stage IV resampled to 1/8 degree-resolution, (bottom left) NLDAS, and (bottom right) TMPA. The dots represent the location of the center of circulation of the storm (the black dots indicate that the storm is extra-tropical).

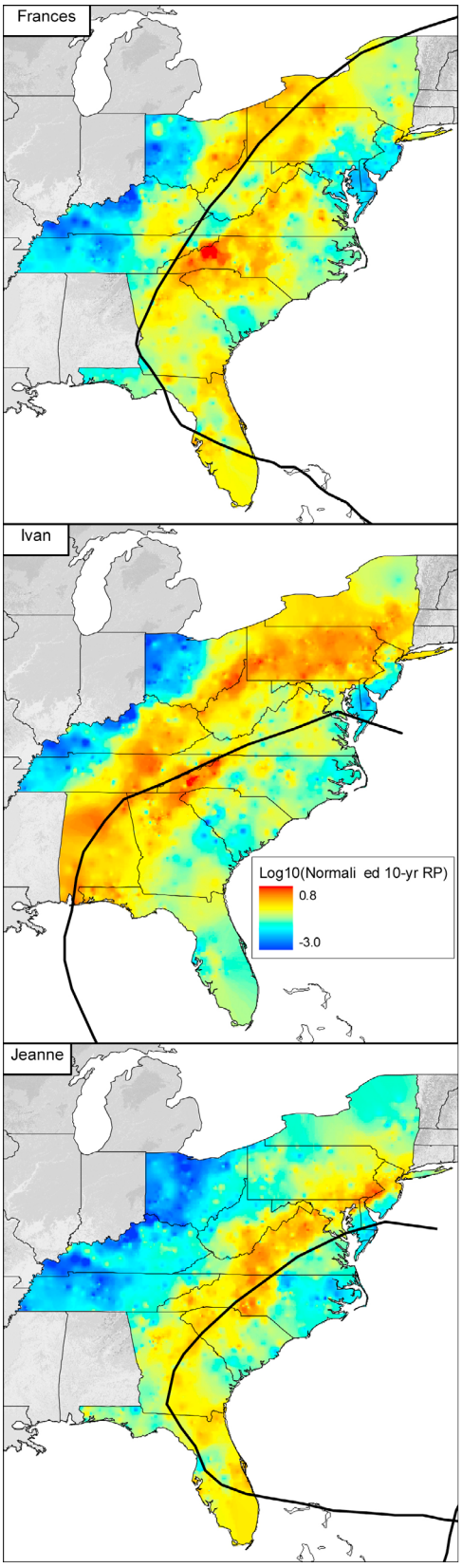

assess whether Stage IV is biased high or NLDAS and TMPA are biased low, we use the runoff values as lower bound. Because runoff values in this area are on the order of 450 mm, we can conclude that in this context Stage IV provides more physically realistic rainfall values than NLDAS and TMPA.

[24] In addition to the runoff values, we have also compared the Stage IV data against eight rain gages, which are part of the U.S. Climate Reference Network (USCRN), in Georgia, North Carolina, South Carolina, and Virginia (see Figure 1 for their locations). We focus only on the Stage IV product because it is the one that is most consistent with the runoff measurements, and also because of the limited impact of the spatial sampling uncertainties at the hourly scale and 4-km pixels (uncertainties associated with the approximation of an areal estimate with a point measurement [e.g., *Villarini et al.*, 2008; *Villarini and Krajewski*, 2008]). There is a very good agreement between the Stage IV and rain gage data, without a consistent departure from the 1:1 line (Figure 5). Moreover, examination of the rainfall time series support the capability of the Stage VI data to capture the peak rainfall associated with the passage of these three hurricanes (figure not shown). *Lonfat et al.* [2007] wrote that "It is not clear how accurate the stage-IV data is for rainfall from landfalling tropical cyclones." Based on the comparisons with respect to the rain gages and the stream gage stations, we think that the Stage IV data provide valuable information towards the characterization of rainfall during these extreme events.

[25] Some of the issues raised for the rainfall storm total for September 2004 (Figure 1) become even more apparent when examining the rainfall storm totals for the different hurricanes. Let us start with Frances (Figure 6), for which we show the rainfall accumulations over the period September 3–11 obtained from the Stage IV (Figure 6, top left), Stage IV resampled to the NLDAS grid (Figure 6, top right), NLDAS (Figure 6, bottom left), and TMPA (Figure 6, bottom right). The largest accumulations are to the right of the track, in particular in northern Florida and out of the coast of Florida and the Carolinas. Over land, all the products tend to agree as far as the location of the heaviest rainfall is concerned. The biggest differences are for the rainfall values. Stage IV tends to have the largest rainfall accumulations and can provide a very detailed description of the rainfall spatial structure. The NLDAS and TMPA show much lower accumulations. To investigate the effects of spatial resolution, we have aggregated the Stage IV to the NLDAS grid: despite the scale coarsening, the resampled Stage IV accumulation is much larger than the NLDAS one, implying that the different resolutions do not explain the differences observed in the storm totals (see also Figure 2). Over open water, the superiority of TMPA is clear, with the

Figure 9. Flood magnitudes for Hurricanes (top) Frances, (middle) Ivan (the storm track is shown until September 19 at 0 UTC), and (bottom) Jeanne normalized with respect to the 10-year flood peak value obtained from the regional relation from *Villarini and Smith* [2010]. For instance, a value of 1 indicates that the flood peak for this event is ten times larger than the regional flood peak with a 10-year return period and the same drainage area. Interpolation is performed using the inverse distance weighting method.

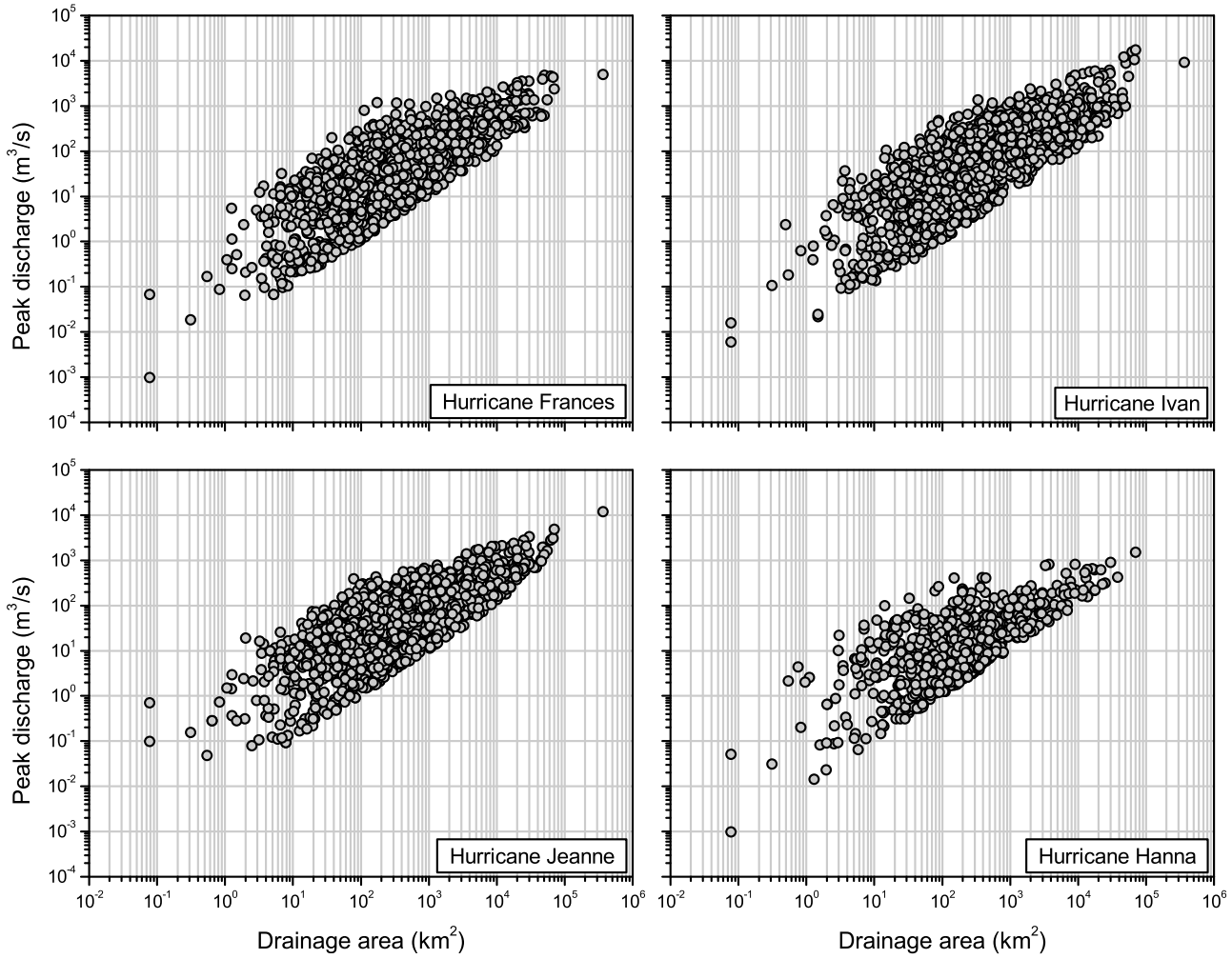

Figure 10. Plots of the peak discharge as a function of drainage area for (top left) Hurricane Frances, (top right) Hurricane Ivan, (bottom left) Hurricane Jeanne, and (bottom right) Hurricane Hanna. A threshold of 0.011 $m^3\ s^{-1}\ km^{-2}$ (1 $ft^3\ s^{-1}\ mi^{-2}$) was adopted. For details about Hurricane Hanna, consult *Smith et al.* [2011].

large rainfall accumulations prior to landfall only partially captured by the Stage IV data. Given its close proximity to the coast, the Stage IV is able to capture the rainfall accumulations out of the coast of the Carolinas.

[26] In Figure 7 we show the rainfall accumulations for Ivan over the period September 13–18. Over this period, Ivan made landfall once in Alabama and then in Florida. Similar to Frances, all of the three rainfall products provide a similar picture of rainfall accumulation over land. At landfall over Alabama, the largest rainfall accumulations are to the right of the track. As it moves inland, the rainfall distribution tends to become more symmetric, with significant rainfall accumulations far from the center of the track. Stage IV provides the most detailed description of the spatial characterization of rainfall, with once again a large rainfall accumulation on the southern end of the Appalachian Mountains. The NLDAS accumulations are much smaller. These differences cannot be solely explained by the coarser resolution, since the re-gridded Stage IV still exhibits much larger accumulations. It is possible that the network of daily rain gages is not dense enough to capture the large spatial variability of the precipitation fields or that the rain gages suffer from undercatchment due to the high winds. TMPA provides good details of the storm in the Gulf of Mexico before the first landfall. Moreover, we can see rainfall accumulations over the North Atlantic Ocean, in particular over the Bahamas. Even though Stage IV can provide information up to about 150 km from the coast, it does not show the pronounced right of the track accumulation before the first landfall as in TMPA due to missing data few hours before landfall.

[27] The third hurricane we have examined is Jeanne, for which we show the rainfall accumulations over the period September 25–30 in Figure 8. All the three products show that most of the storm total rainfall accumulation was to the right of the track in Florida. As the hurricane moves inland, the storm total accumulation becomes more symmetric. According to the Stage IV data, we have very large accumulations in Florida around Palm Bay and Jacksonville. These features are consistent across the different products, even though it is possible that some of the very large values

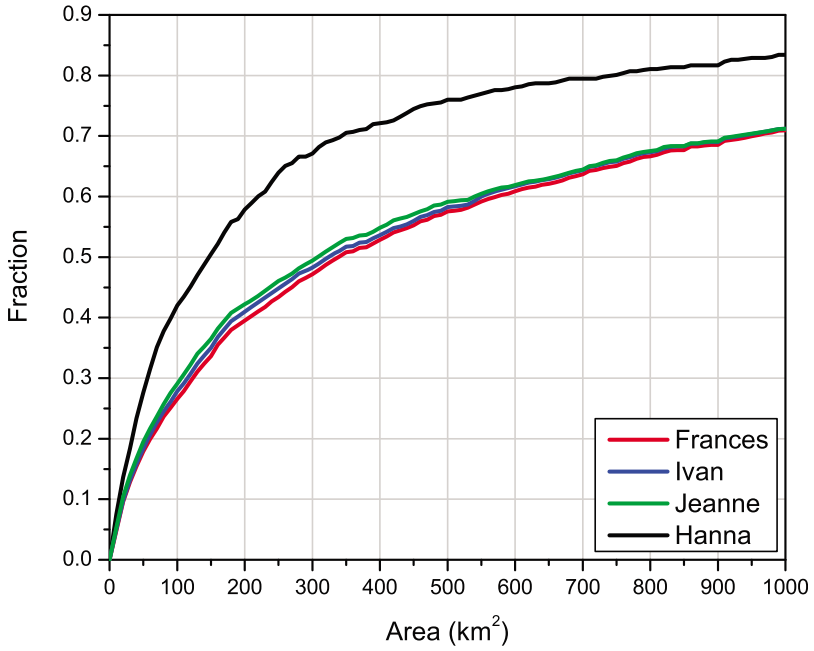

Figure 11. Plot of the fraction of the total stations exceeding the threshold of 0.011 $m^3\ s^{-1}\ km^{-2}$ (1 $ft^3\ s^{-1}\ mi^{-2}$) as a function of drainage area.

for the Stage IV around the Jacksonville area could be associated with radar artifacts, such as ground clutter and anomalous propagation [e.g., *Villarini and Krajewski*, 2010]. NLDAS tends to consistently underestimate rainfall with respect to the Stage IV data. TMPA can provide a good view of the rainfall accumulations in open ocean and before landfall. This is only partially captured by the Stage IV data.

[28] Based on these analyses, we suggest using the Stage IV data when evaluating the temporal and spatial evolution of landfalling tropical cyclones. This product has both fine spatial and temporal scales, and can provide information about the rainfall distribution up to about 150 km out in the sea. Moreover, its estimates are more consistent with the measured runoff and rain gage values. For these reasons, in Section 3.3 we focus on the Stage IV to describe the evolution of rainfall for these three hurricanes.

3.2. Runoff and Peak Streamflow Analyses of the Three Hurricanes

[29] Heavy rainfall associated with these three events was responsible for flooding over large portions of the eastern U.S. Apart from annual maximum peak discharge data, USGS maintains and publishes discharge time series with fine temporal resolution (between 1 and 60 minutes) for approximately the past 20 years. We can use these data to investigate the flood extent for these three events and their relation with the rainfall distribution.

[30] When examining flood peaks over a large area, one complicating factor is the different drainage areas of these catchments. It would be useful to relate the flood magnitude for these events to a reference regional value. To accomplish this [see *Smith et al.*, 2011] we have normalized the peaks for each catchment and event by the 10-year flood peak value obtained from the regional relation of *Villarini and Smith* [2010]. Given a drainage area and a return period, the power-law relation from *Villarini and Smith* [2010] provides the regional flood peak for that drainage area and return period. We develop normalized flood maps by interpolating normalized flood peak values from USGS gaging stations.

[31] We have summarized the results for the three hurricanes in Figure 9, where we used 2383 USGS stations for Frances, 2396 for Ivan, and 2181 for Jeanne. A value of 1 indicates that the flood peak at the streamgage station is 10 times larger than the 10-year flood peak value for a catchment with the same drainage area. Large scale features of the flood maps reflect large scale features of rainfall fields. For Frances, most of the flooding affected areas to the right of the track, and in particular North Carolina. The flooding extent for Ivan covers a larger area, from Alabama to New York. This larger spatial extent reflects the larger spatial extent of heavy rainfall (Figure 7). The results for Jeanne are consistent with the rainfall patterns in Figure 8, in which we have larger rainfall accumulations along the Appalachian Mountains. From the maps in Figure 9 we can also highlight the large spatial structure associated with these flooding events. Flood peaks at nearby locations tend to have similar normalized peak values, indicating that a flood model at the regional scale should move away from "at-site" analyses and aim at incorporating the spatial correlation of flood peaks.

[32] We have examined the scaling properties of flood peaks following analyses by *Smith et al.* [2011]. From each streamgage station and hurricane, we have plotted the maximum discharge as a function of drainage area (Figure 10). We have set a threshold of 0.011 $m^3\ s^{-1}\ km^{-2}$ (1 $ft^3\ s^{-1}\ mi^{-2}$), meaning that we have excluded stations for which the peak discharge divided by drainage area was smaller than 0.011 $m^3\ s^{-1}\ km^{-2}$ (1 $ft^3\ s^{-1}\ mi^{-2}$). These analyses indicate that scaling properties of Frances, Ivan and Jeanne are similar, but contrast with those of Hanna (see also Figure 11).

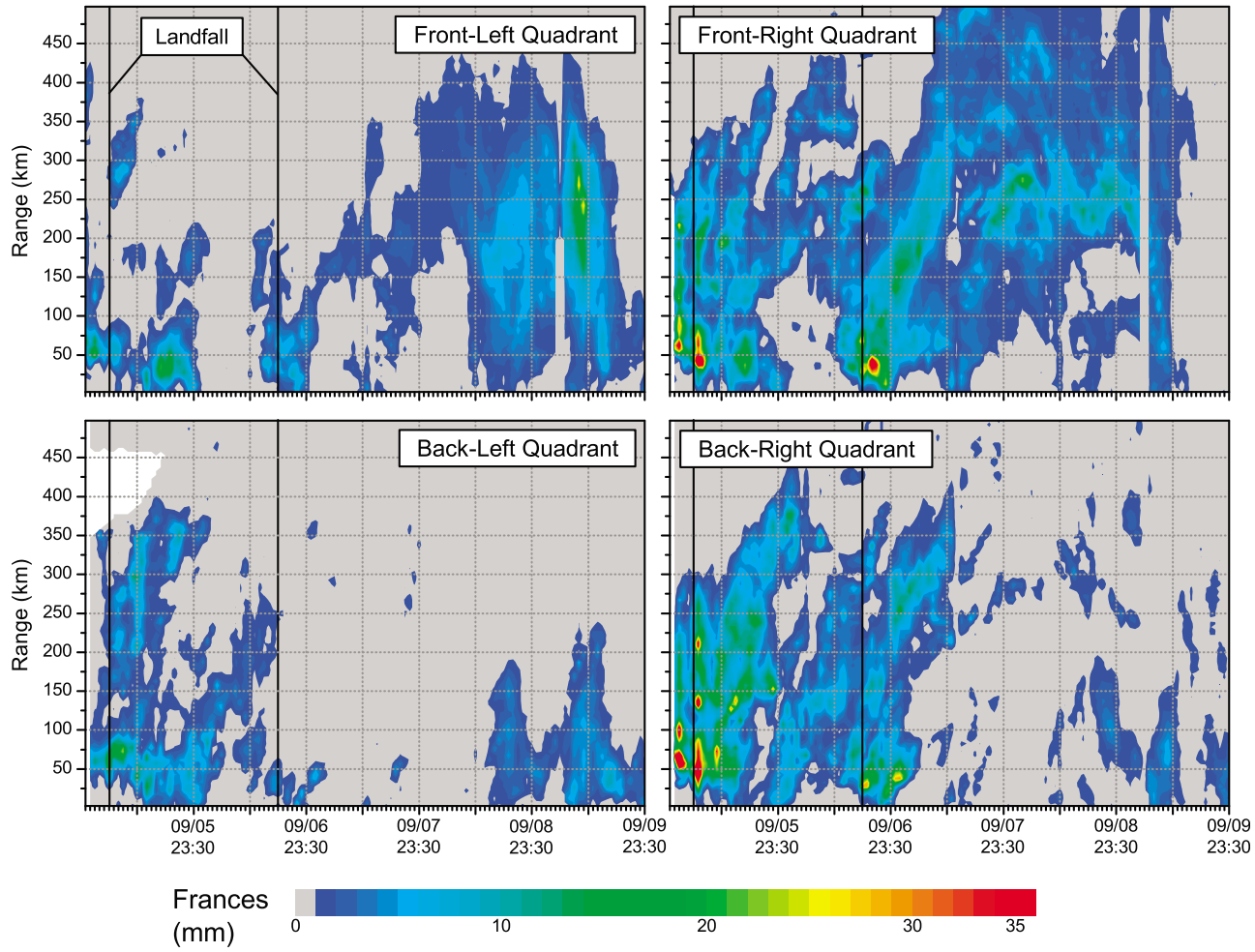

Figure 12. Rainfall distribution as a function of distance from the center of circulation during the landfall of Hurricane Frances based on the Stage IV data. The four quadrants are defined with respect to the direction of propagation of the storm.

The numbers of USGS gaging stations with flood peaks exceeding the 1 $ft^3\ s^{-1}\ mi^{-2}$ threshold are similar for Frances (1374), Ivan (1462) and Jeanne (1275), but much larger than the 638 stations with peak greater than 1 1 $ft^3\ s^{-1}\ mi^{-2}$ for Hanna. Hurricane Hanna exhibited the most significant flooding at smaller drainage areas (Figure 11). In Figure 11, we illustrate the concentration of small-basin flooding from Hurricane Hanna by plotting the fraction of the total stations exceeding the 1 $ft^3\ s^{-1}\ mi^{-2}$ threshold as a function of drainage area. The results for the three 2004 storms are virtually identical with approximately 50% of stations less than 300 km^2. For Hanna the corresponding drainage area accounting for 50% of stations is less than 150 km^2. Future studies will examine whether there are systematic scaling properties of flood peaks that can be attributed to specific classes of landfalling tropical cyclones.

3.3. Evolution of Rainfall Distribution Over Land

[33] In this section we provide a detailed description of the azimuthally averaged rainfall distribution as a function of distance from the center of circulation. Information about the storm track is provided by the HURDAT database [*Jarvinen et al.*, 1984; *Neumann et al.*, 1993; *MacAdie et al.*, 2009], for which the location of the center of the tropical cyclone is available every six hours. To obtain the location of the center of circulation at the temporal resolution of the Stage IV data, we linearly interpolate the six-hourly data from the HURDAT down to the hourly scale. In this way, we are able to describe the rainfall distribution every hour. When computing the radial distribution, instead of averaging over a 360° azimuth, we consider four different quadrants: front−left, front−right, back−left, and back−right. Rather than distinguishing them with respect to the Geographic North, we use a Lagrangian approach, in which we follow the storm and divide the domain into four different quadrants with respect to the direction of propagation of the storm. This type of analysis can provide very detailed and valuable information about the temporal evolution of rainfall in landfalling tropical cyclones and hurricanes.

[34] In Figure 12 we show the rainfall evolution of Frances. We indicate the approximate time of the two landfalls with the two vertical lines. These plots provide a wealth of details and also highlight the complexity in the rainfall fields in a landfalling hurricane. The rainfall accumulation

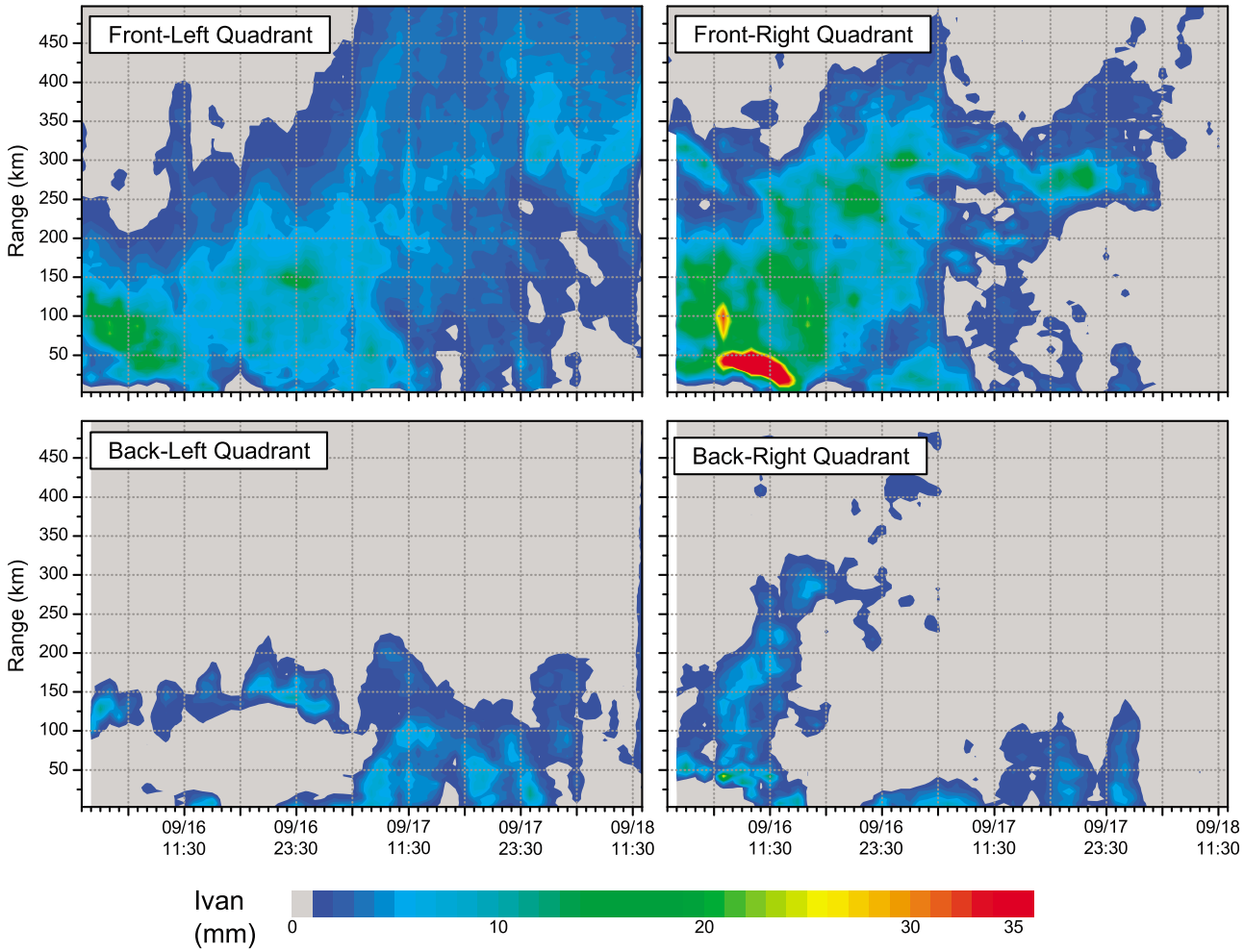

Figure 13. Rainfall distribution as a function of distance from the center of circulation during the landfall of Hurricane Ivan based on the Stage IV data. The four quadrants are defined with respect to the direction of propagation of the storm.

was mostly to the right of the track. Before landfall, the maximum rainfall tends to be concentrated within 50 km and 100 km from the center of circulation. Around landfall, the maximum in rainfall distribution tends to move towards the center of circulation, indicating the collapse of the eye. As the storm moves inland, the peak rainfall becomes smaller and the rainfall distribution tends to then move away from the center. Compared to other studies [e.g., *Jiang et al.*, 2008b], the pattern is qualitatively similar while the values are different, probably because of the different rainfall products used and the fact that we are dealing with a specific event rather than examining rainfall averaged over multiple storms. We can also see how the rainfall affects a very large area (up to 500 km from the center of circulation). This type of plots can also provide valuable information about the presence of outer rain bands.

[35] Ivan made its first landfall in Alabama and then moved inland (the time series start right after landfall due to lack of data for few hours before landfall). We do not see all the variability exhibited by Frances (Figure 13). After landfall, the maximum rainfall moves from about 50 km from the center of circulation towards the center, in association with the collapse of the eye. These results are in agreement with findings in previous studies examining the different radial distribution of rainfall over oceans and over land. This is particularly evident for the front-right quadrant, where the maximum rainfall moves closer to the center of circulation during landfall. The largest rainfall values right after landfall are concentrated to the right of the track. After interacting with the Appalachian Mountains, however, the rainfall distribution is mostly to the left of the track, affecting areas up to 500 km from the center of the storm (see also discussions by *Atallah and Bosart* [2003], *Colle* [2003], and *Atallah et al.* [2007], among others). By focusing on the front-right quadrant we can also see a rain band between 250 and 300 km from the center of the storm.

[36] Jeanne showed a structure more similar to Ivan than Frances (Figure 14). Right before landfall, the maximum rainfall is concentrated between 50 km and 100 km from the center of circulation. As the storm moves inland, the maximum rainfall moves towards the center of the storm. The largest rainfall values are at first to the right of the track. During its march inland, increasingly larger areas are affected by its rainfall, with the rainfall distribution moving

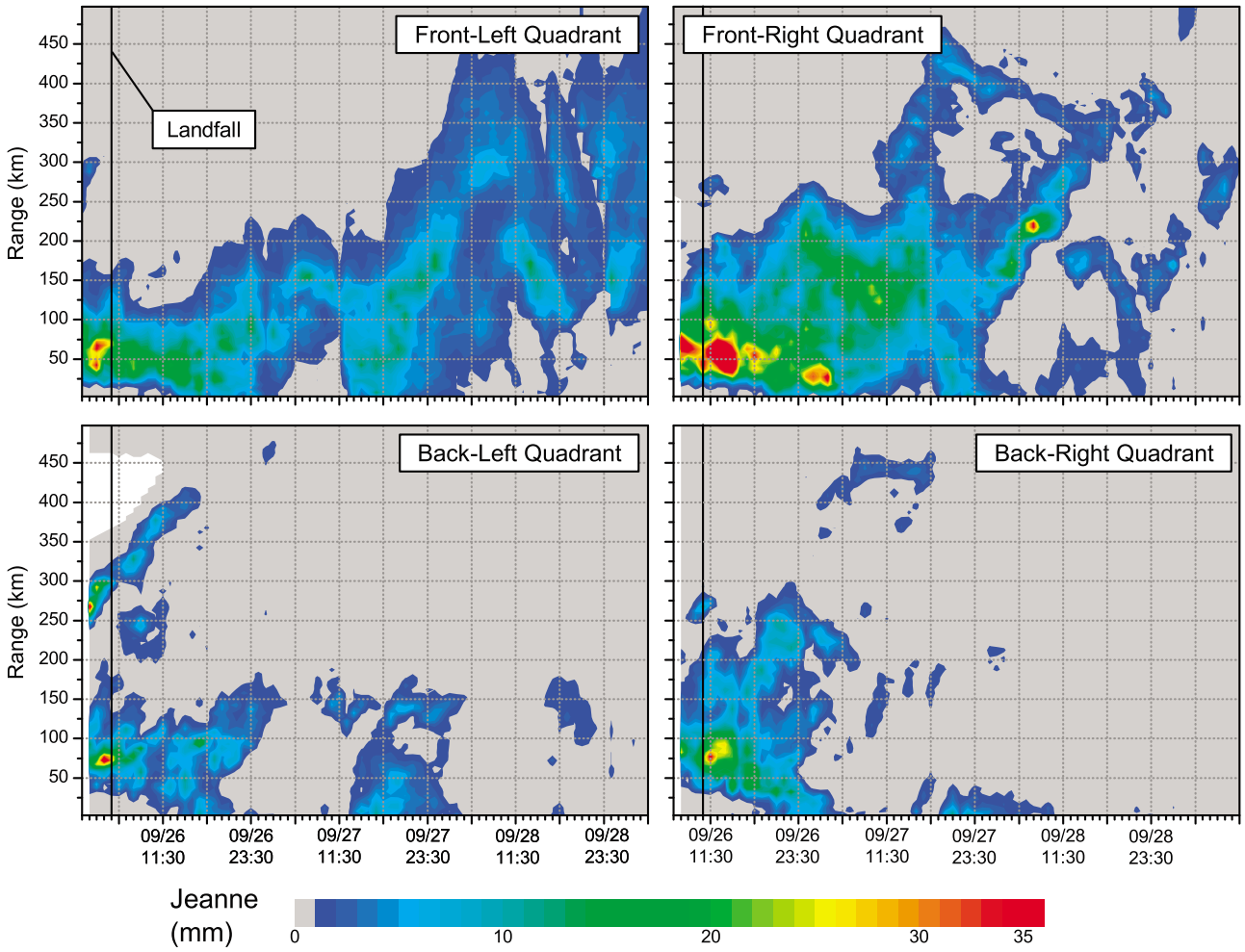

Figure 14. Rainfall distribution as a function of distance from the center of circulation during the landfall of Hurricane Jeanne based on the Stage IV data. The four quadrants are defined with respect to the direction of propagation of the storm.

to the left of the track. From this plot, we can see rain bands at distances larger than 200 km from the center of the storm.

[37] NLDAS data are also available every hour. For comparison, we want to show the results that we would obtain when examining the radial distribution of rainfall using NLDAS. We focus on Ivan (Figure 15) but the same conclusions are valid for Frances and Jeanne. Even though the results obtained using NLDAS are in qualitative agreement with those from the Stage IV, the rainfall values are much smaller, as expected from the comparison of the storm totals. Moreover, we only have data over land, which does not allow examining the development of the rainfall field prior to landfall. From Figure 15 we can see large areas with missing data, which affect our capability of tracking the storm transition from water to land. Once well inland, we have a better qualitative and quantitative agreement between Stage IV and NLDAS.

[38] Based on these three events, we can observe some common features (e.g., collapse of the eye after landfall and corresponding shift in the location of the maximum in rainfall distribution). To highlight these common characteristics, we have averaged the rainfall distribution for the three events using the time of landfall as common initial time reference (Figure 16). Since Frances made landfall twice, we have considered it as two events (before and after the second landfall). Several interesting features can be observed. For these events, the largest rainfall accumulations are to the right of the storm track, in particular in the front-right quadrant. Within about 10–15 hours after land we observe the collapse of the eye and the maximum rainfall shifting towards the center of the storm. We can then observe the formation of outer rain bands and rainfall at more than 400 km from the storm. These results provide important indications of the characteristics shared by these three hurricanes. These features should be taken into account when developing a model to describe rainfall distribution in tropical cyclones during landfall.

4. Conclusions

[39] The main findings of this study can be summarized as follows:

[40] 1. Three gridded rainfall products (Stage IV, NLDAS, and TMPA) were evaluated for assessing the structure and

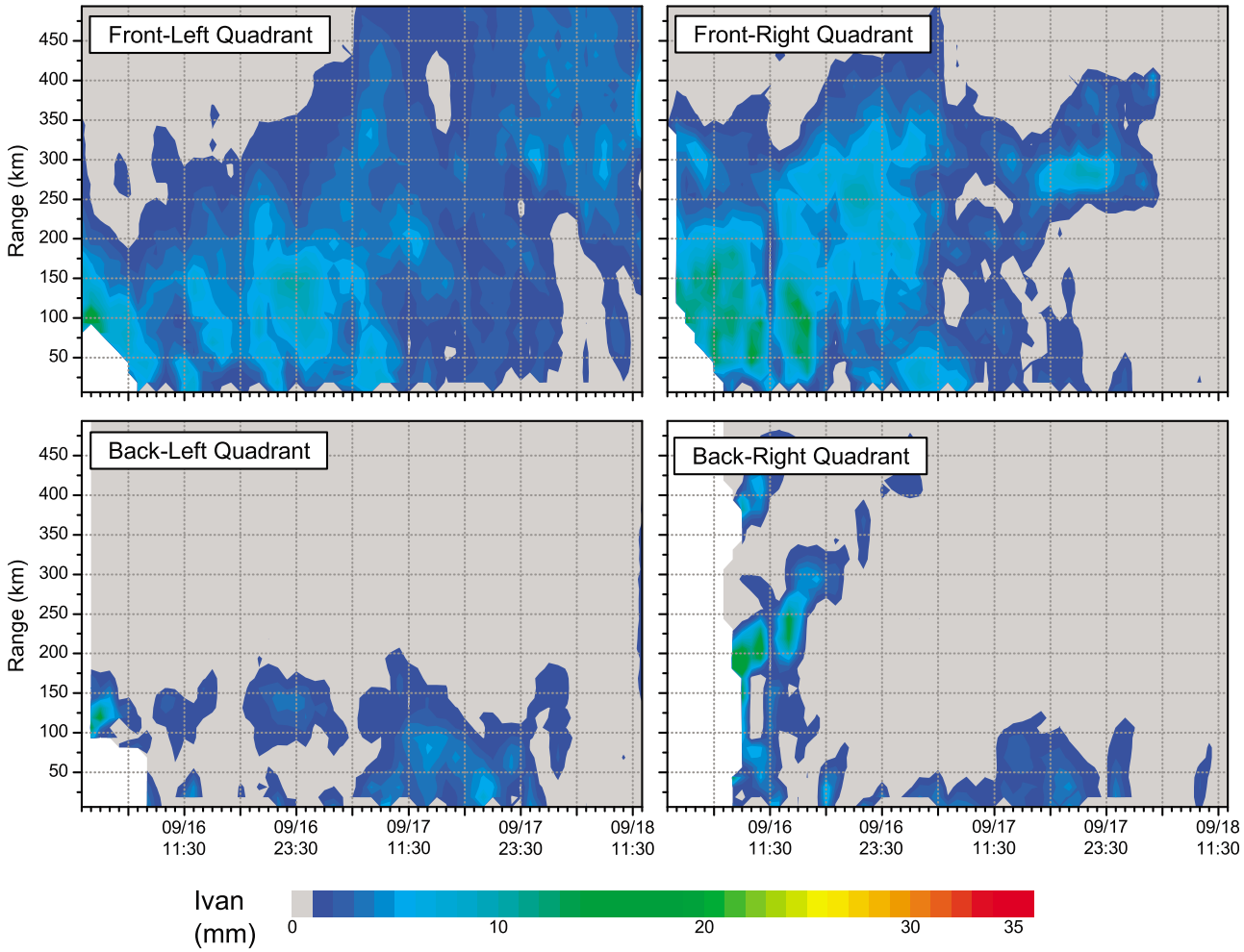

Figure 15. Rainfall distribution as a function of distance from the center of circulation during the landfall of Hurricane Ivan based on the NLDAS data. The four quadrants are defined with respect to the direction of propagation of the storm.

evolution of rainfall for landfalling tropical cyclones. Each of these products has strengths and weaknesses. TMPA is based on satellite data (and bias-corrected with rain gages) and is able to provide description of the storms over both land and ocean. Its spatial and temporal resolutions (three hourly and 0.25-degree lat/lon), however, are too coarse to capture the high spatio-temporal variability of rainfall associated with a tropical cyclone during landfall. NLDAS is a rain gage-only product with higher spatial and temporal resolutions compared to TMPA (hourly and 0.125-degree lat/lon). It can, however, provide rainfall estimates only over land, which does not allow analysis of the storm evolution before landfall. Moreover, its rainfall estimates were smaller than those from the other products. Finally, Stage IV is obtained by merging ground-based radar data and rain gage measurements. It is characterized by the highest spatial and temporal resolutions (approximately 4-km and hourly), and can provide detailed information of the rainfall evolution prior to landfall (up to about 150 km from the coast). Given all the strengths and weaknesses of these products, we conclude that the Stage IV data is the best suited to study rainfall distribution for landfalling tropical cyclones.

[41] 2. We use discharge observations from more than 2000 USGS stream gaging stations to examine the spatial structure and scaling properties of flood peaks from tropical cyclones. Analyses demonstrate the feasibility of "data-driven" approaches to spatial flood hazard assessment based on tropical cyclone tracks and USGS stream gaging observations.

[42] 3. We present a Lagrangian method for characterizing temporal evolution of the spatial structure of rainfall from tropical cyclones. Analyses of the 2004 hurricanes illustrate: (1) the rapidly changing rainfall structure at landfall; (2) evolving contributions of the eyewall convection inner rain bands and outer rain bands; and (3) left-of-track, right-of-track contrasts in rainfall structure [e.g., *Atallah et al.* [2007] and the pronounced effects of terrain. Evolving rainfall structure is linked to spatial extremes of flooding (item 2 above).

[43] 4. In future studies we are planning on using Stage IV data and USGS stream gage data to analyze a large sample of U.S. landfalling tropical cyclones starting from the 1996 season. This expanded data set will then be instrumental in

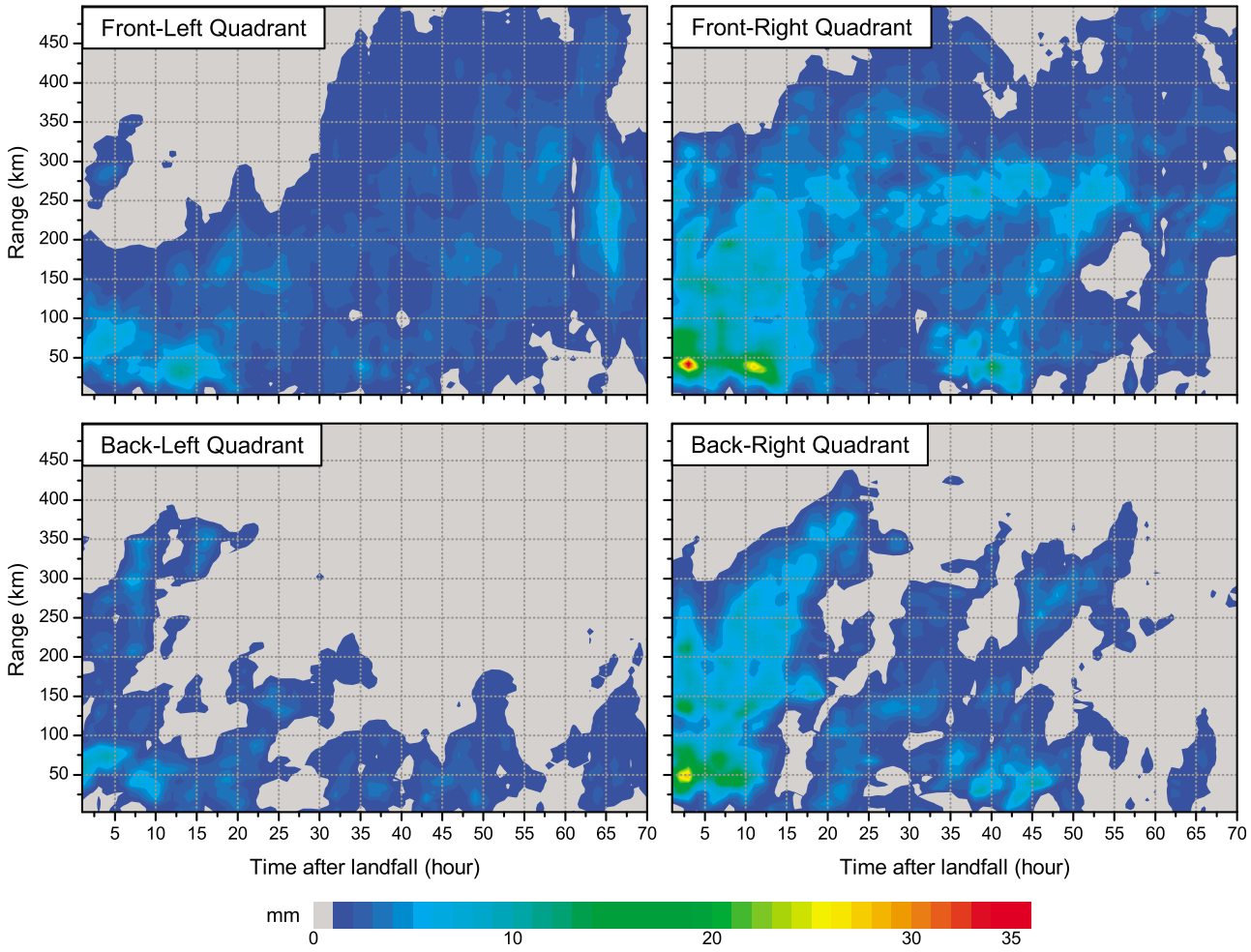

Figure 16. Rainfall distribution as a function of distance from the center of circulation based on the Stage IV data computed by averaging the radial distributions from Figures 12–14. The four quadrants are defined with respect to the direction of propagation of the storm.

the development of a model to quantify flood risk from tropical cyclones.

[44] **Acknowledgments.** This research was funded in part by the Willis Research Network, the National Science Foundation (grant EAR-0847347 and grant CMMI-0653772), and NASA.

References

American Meteorological Society (AMS) (2000), Policy statement: Hurricane research and forecasting, *Bull. Am. Meteorol. Soc.*, *6*, 1341–1346.

Atallah, E., and L. F. Bosart (2003), The extratropical transition and precipitation distribution of Hurricane Floyd (1999), *Mon. Weather Rev.*, *131*, 1063–1081.

Atallah, E., L. F. Bosart, and A. R. Aiyyer (2007), Precipitation distribution associated with landfalling tropical cyclones over the Eastern United States, *Mon. Weather Rev.*, *135*, 2185–2206.

Baldwin, M. E., and K. E. Mitchell (1998), Progress on the NCEP hourly multi-sensor U.S. precipitation analysis for operation and GCIP research, paper presented at 13th Conference on Hydrology, Am. Meteorol. Soc., Long Beach, Calif.

Blackwell, K. G. (2000), The evolution of Hurricane Danny (1997) at landfall: Doppler-observed eyewall replacement, vortex contraction/intensification, and low-level wind maxima, *Mon. Weather Rev.*, *128*, 4002–4016.

Cerveny, R. S., and L. E. Newman (2000), Climatological relationships between tropical cyclones and rainfall, *Mon. Weather Rev.*, *128*, 3329–3336.

Changnon, S. A. (2009), Characteristics of severe Atlantic hurricanes in the United States: 1949–2006, *Nat. Hazards*, *48*, 329–337.

Colle, B. A. (2003), Numerical simulations of the extratropical transition of Floyd (1999): Structural evolution and responsible mechanisms for the heavy rainfall over the northeast U.S., *Mon. Weather Rev.*, *131*, 2905–2926.

Compo, G. P., J. S. Whitaker, and P. D. Sardeshmukh (2006), Feasibility of a 100 year reanalysis using only surface pressure data, *Bull. Am. Meteorol. Soc.*, *87*, 175–190.

Compo, G. P., et al. (2011), The Twentieth Century Reanalysis Project, *Q. J. R. Meteorol. Soc.*, *137*, 1–28.

Curtis, S., T. W. Crawford, and S. A. Lecce (2007), A comparison of TRMM to other basin-scale estimates of rainfall during the 1999 Hurricane Floyd flood, *Nat. Hazards*, *43*, 187–198.

Ebert, E. E., M. Turk, S. J. Kusselson, J. Yang, M. Seybold, P. R. Keehn, and R. J. Kuligowski (2011), Ensemble tropical rainfall potential (eTRaP) forecasts, *Weather Forecast.*, *26*, 213–224.

Elsberry, R. L. (2002), Predicting hurricane landfall precipitation: Optimistic and pessimistic views from the Symposium on Precipitation Extremes, *Bull. Am. Meteorol. Soc.*, *83*, 1333–1339.

Ferraro, R., P. Pellegrino, M. Turk, W. Chen, S. Qui, R. J. Kuligowski, S. Kusselson, A. Irving, S. Kidder, and J. Knaff (2005), The Tropical Rainfall Potential (TRaP) technique. Part II: Validation, *Weather Forecast.*, *20*, 465–475.

Franklin, J. L., R. J. Pasch, L. A. Avila, J. L. Beven II, M. B. Lawrence, S. R. Stewart, and E. S. Blake (2006), Atlantic hurricane season of 2004, *Mon. Weather Rev.*, *134*, 981–1025.

Glitto, P., and B. Choy (1997), A comparison of WSR-88D storm total precipitation perfromance during two tropical systems following changes

to the multiplicative bias and upper reflectivity threshold, *Weather Forecast.*, *12*, 459–471.
Hellin, J., M. Haigh, and F. Marks (1999), Rainfall characteristics of Hurricane Mitch, *Nature*, *399*, 316.
Huffman, G. J., R. F. Adler, D. T. Bolvin, G. Gu, E. J. Nelkin, K. P. Bowman, Y. Hong, E. F. Stocker, and D. B. Wolff (2007), The TRMM Multisatellite Precipitation Analysis (TMPA): Quasi-global, multiyear, combined-sensor precipitation estimates at fine scale, *J. Hydrometeorol.*, *8*, 38–55.
Jarvinen, B. R., C. J. Neumann, and M. A. S. Davis (1984), A tropical cyclone data tape for the North Atlantic Basin, 1886–1983: Contents, limitations, and uses, *Tech. Memo NWS NHC 22*, NOAA, Boulder, Colo.
Javier, J. R. N., J. A. Smith, M. L. Baeck, and G. Villarini (2010), Flash flooding in the Philadelphia metropolitan region, *J. Hydrol. Eng.*, *15*(1), 29–38.
Jiang, H. Y., J. B. Halverson, and J. Simpson (2008a), On the differences in storm rainfall from hurricanes Isidore and Lili. Part I: Satellite observations and rain potential, *Weather Forecast.*, *23*(1), 29–43.
Jiang, H. Y., J. B. Halverson, J. Simpson, and E. J. Zipser (2008b), Hurricane "Rainfall Potential" derived from satellite observations aids overland rainfall prediction, *J. Appl. Meteorol. Climatol.*, *47*(4), 944–959.
Jones, P. W. (1999), First- and second-order conservative remapping schemes for grids in spherical coordinates, *Mon. Weather Rev.*, *127*, 2204–2210.
Kidder, S. Q., S. J. Kusselson, J. A. Knaff, R. R. Ferraro, R. J. Kuligowski, and M. Turk (2005), The Tropical Rainfall Potential (TRaP) technique. Part I: Description and examples. *Weather Forecast.*, *20*, 456–464.
Kimball, S. K. (2008), Structure and evolution of rainfall in numerically simulated landfalling hurricanes, *Mon. Weather Rev.*, *136*, 3822–3847.
Langousis, A., and D. Veneziano (2009a), Long-term rainfall risk from tropical cyclones in coastal areas, *Water Resour. Res.*, *45*, W11430, doi:10.1029/2008WR007624.
Langousis, A., and D. Veneziano (2009b), Theoretical model of rainfall in tropical cyclones for the assessment of long-term risk, *J. Geophys. Res.*, *114*, D02106, doi:10.1029/2008JD010080.
Lin, N., J. A. Smith, G. Villarini, T. P. Marchok, and M. L. Baeck (2010), Modeling extreme rainfall, winds, and surge from Hurricane Isabel (2003), *Weather Forecast.*, *25*(5), 1342–1361.
Lin, Y., and K. E. Mitchell (2005), The NCEP Stage II/IV hourly precipitation analyses: Development and applications, paper presented at 19th Conference on Hydrology, Am. Meteorol. Soc., San Diego, Calif.
Lonfat, M., F. D. Marks, and S. S. Chen (2004), Precipitation distribution in tropical cyclones using the Tropical Rainfall Measuring Mission (TRMM) microwave imager: A global perspective, *Mon. Weather Rev.*, *135*, 1645–1660.
Lonfat, M., R. Rogers, T. Marchok, and F. D. Marks (2007), A parametric model for predicting hurricane rainfall, *Mon. Weather Rev.*, *135*, 3086–3097.
MacAdie, C. J., C. W. Landsea, C. J. Neumann, J. E. David, E. Blake, and G. R. Hammer (2009), Tropical cyclones of the North Atlantic Ocean, 1851–2006, technical memo, Natl. Clim. Data Cent., Asheville, N. C.
Marchok, T., R. Rogers, and R. Tuleya (2007), Validation schemes for tropical cyclone quantitative precipitation forecasts: Evaluation of operational models for U.S. landfalling cases, *Weather Forecast.*, *22*, 726–746.
Matyas, C. J. (2009), A spatial analysis of radar reflectivity regions within Hurricane Charley (2004), *J. Appl. Meteorol. Climatol.*, *48*, 130–142.
Matyas, C. J., and M. Cartaya (2009), Comparing the rainfall patterns produced by Hurricanes Frances (2004) and Jeanne (2004) over Florida, *Southeast. Geogr.*, *49*(2), 132–156.
Medlin, J. M., S. K. Kimball, and K. G. Blackwell (2007), Radar and rain gauge analysis of the extreme rainfall during Hurricane Danny's (1997) landfall, *Mon. Weather Rev.*, *135*, 1869–1888.
Mitchell, K. E., et al. (2004), The multi-institution North American Land Data Assimilation System (NLDAS): Utilizing multiple GCIP products and partners in a continental distributed hydrological modeling system, *J. Geophys. Res.*, *109*, D07S90, doi:10.1029/2003JD003823.
Neumann, C. J., B. R. Jarvinen, C. J. McAdie, and J. D. Elms (1993), Tropical cyclones of the North Atlantic Ocean, technical memo, Natl. Clim. Data Cent., Asheville, N. C.
Padoan, S. A., M. Ribatet, and S. A. Sisson (2010), Likelihood-based inference for max-stable processes, *J. Am. Stat. Assoc.*, *105*, 263–277.
Pielke, R. A., J. Gratz, C. W. Landsea, D. Collins, M. A. Saunders, and R. Musulin (2008), Normalized hurricane damage in the United States: 1900–2005, *Nat. Hazards Rev.*, *9*(1), 29–42.
Rao, G. V., and P. D. MacArthur (1994), The SSM/I estimated rainfall amounts of tropical cyclones and their potential in predicting the cyclone intensity changes, *Mon. Weather Rev.*, *122*, 1568–1574.
Rappaport, E. N. (2000), Loss of life in the United States associated with recent Atlantic tropical cyclones, *Bull. Am. Meteorol. Soc.*, *81*, 2065–2073.
Reed, S. M., and D. R. Maidment (1999), Coordinate transformation for using NEXRAD data in GIS-based hydrologic modeling, *J. Hydrol. Eng.*, *4*(2), 174–182.
Rodgers, E. B., and R. F. Adler (1981), Tropical cyclone rainfall characteristics as determined from a satellite passive microwave radiometer, *Mon. Weather Rev.*, *109*, 506–521.
Rodgers, E. B., and H. F. Pierce (1995), A satellite observational study of precipitation characteristics in western Pacific tropical cyclones, *J. Appl. Meteorol.*, *34*, 2587–2599.
Rodgers, E. B., S. W. Chang, and H. F. Pierce (1994), A satellite observational and numerical study of precipitation characteristics in western North Atlantic tropical cyclones, *J. Appl. Meteorol.*, *33*, 129–139.
Smith, J. A., G. Villarini, and M. L. Baeck (2011), Mixture distributions and the climatology of extreme rainfall and flooding in the eastern US, *J. Hydrometeorol.*, *12*(2), 294–309.
Sturdevant-Rees, P. L., J. A. Smith, J. Morrison, and M. L. Baeck (2001), Tropical storms and the flood hydrology of the Central Appalachians, *Water Resour. Res.*, *37*(8), 2143–2168.
Tuleya, R. E., M. DeMaria, and R. J. Kuligowski (2007), Evaluation of GFDL and simple statistical model of rainfall for U.S. landfalling tropical storms, *Weather Forecast.*, *22*, 56–70.
Villarini, G., and W. F. Krajewski (2008), Empirically-based modeling of spatial sampling uncertainties associated with rainfall measurements by rain gauges, *Adv. Water Resour.*, *31*(7), 1015–1023.
Villarini, G., and W. F. Krajewski (2010), Review of the different sources of uncertainty in single-polarization radar-based estimates of rainfall, *Surv. Geophys.*, *31*, 107–129.
Villarini, G., and J. A. Smith (2010), Flood peak distributions for the eastern United States, *Water Resour. Res.*, *46*, W06504, doi:10.1029/2009WR008395.
Villarini, G., P. V. Mandapaka, W. F. Krajewski, and R. J. Moore (2008), Rainfall and sampling errors: A rain gauge perspective, *J. Geophys. Res.*, *113*, D11102, doi:10.1029/2007JD009214.
Villarini, G., J. A. Smith, M. L. Baeck, P. Sturdevant-Rees, and W. F. Krajewski (2010), Radar analyses of extreme rainfall and flooding in urban drainage basins, *J. Hydrol.*, *381*(3–4), 266–286.
Yokoyama, C., and Y. N. Takayabu (2008), A statistical study on rain characteristics of tropical cyclones using TRMM satellite data, *Mon. Weather Rev.*, *136*, 3848–3862.

M. L. Baeck, J. A. Smith, and G. Villarini, Department of Civil and Environmental Engineering, Princeton University, Engineering Quadrangle, Princeton, NJ 08540, USA. (gvillari@princeton.edu)

T. Marchok and G. A. Vecchi, Geophysical Fluid Dynamics Laboratory, National Oceanic and Atmospheric Administration, Princeton Forrestal Campus, Route 1, PO Box 308, Princeton, NJ 08542-0308, USA.